

### INTRODUCTION

Acoustic waves in the sun are separated into two categories: global and local. Global oscillations are excited through convection, and resonate in the solar interior. As with all resonant media, propagation of these acoustic waves is limited to specific frequencies for a given wavenumber. These modes are easily distinguished in l-v diagrams, such as in figure 1. Global modes dominate the spectrum in the 2-5 mHz range. Local oscillations, so-called “sunquakes”, are usually excited by particularly strong flares and can be observed as ring-shaped waves propagating away from the point of impact. The propagation is best displayed in a time-distance diagram, where a slit passing from the source to some distance away. Distance is displayed on the x-axis, and the time-series is plotted along the y-axis; an example is shown in figure 1, showing the sunquake induced by the Sept 2017 X-class flare (Sharykin and Kosovichev, 2018).

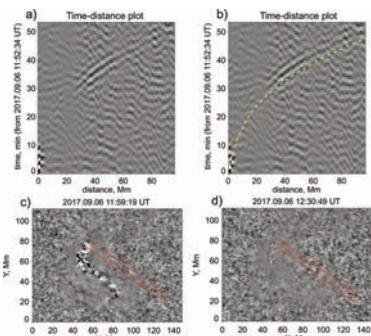


Figure 1: Time-distance diagram of the sunquake produced by the Sept 2017 X-class flare (top row). Two time series Dopplergrams of the flare which produced the sunquake, with the slit used for the TD diagrams in red (bottom row).

We construct a hydrodynamic model to determine whether sunquakes are excited above or below the solar surface. Additionally, we aim to gain insight into what type of perturbation causes these sunquakes.

### MOTIVATION

In the past few decades, helioseismology has played an important role in studying the solar interior. It remains one of the few methods able to glimpse the structure of our Sun. Recent studies (Itonidis and Zhao, 2009; Braun, 2018; etc.) have moved from away from examining the static structure of the Sun towards a better understanding of emerging flux and active regions. Helioseismology allows us to observe the emerging flux by measuring travel time differences between certain frequencies of waves. The experimental procedure is clear, but it is difficult to verify the accuracy of such techniques since validation data is unavailable (we cannot know exactly the density, temperature, etc. of such submerged regions.)

The constructed model can be used to verify the shifted travel time method by “inserting” a region of increased density and sound speed and observing changes to the background state.

### GOVERNING EQUATIONS AND METHOD

We consider linear (Eulerian) perturbations to the equations for mass continuity, momentum, and adiabaticity. We can separate the radial and angular dependence of the variables by using a spherical harmonic decomposition. In this way, the governing equations take the form:

$$\frac{\partial \bar{p}_l}{\partial t} + \frac{\partial v_{r,l}}{\partial r} + v_{r,l} \frac{\partial \ln \rho_0}{\partial r} - \frac{L^2 v_{h,l}}{r} = 0$$

$$\frac{\partial \bar{P}_l}{\partial t} + \gamma \left[ v_{r,l} \frac{N^2}{g} + \frac{\partial v_{r,l}}{\partial r} + v_{r,l} \frac{\partial \ln \rho_0}{\partial r} + \frac{L^2 v_{h,l}}{r} \right] = 0$$

$$\frac{\partial v_{r,l}}{\partial t} = -\frac{1}{\rho_0} \frac{\partial P'_l}{\partial r} + \bar{p}_l g_0 + \frac{F_{r,l}}{\rho_0}$$

$$\frac{\partial v_{h,l}}{\partial t} = -\frac{1}{\rho_0} \left( \frac{P'_l}{r} + F_{h,l} \right)$$

Where subscript l denotes angular degree, overbarred variables indicate a normalized perturbation,  $F_h$  and  $F_r$  correspond to external forces, and  $L^2 = l(l+1)$ . Since sunquake propagation is circularly symmetric, we neglect azimuthal dependence and the spherical harmonics simplify to Associated Legendre Polynomials. The equations are advanced in time through a forward-time, central space scheme (FTCS) with a staggered mesh.

### RESULTS

To ensure the accuracy of the model, we first compare the simulated power spectrum to the observed spectrum (figure 2). The observed power spectrum data are obtained from the MDI instrument aboard SOHO.

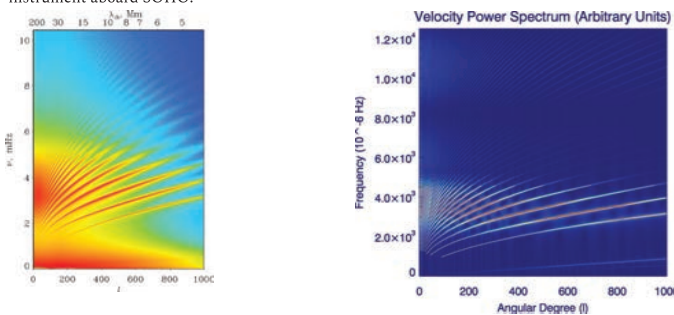


Figure 2: Observed power spectrum at right from a 6-day time series. Note the ridge-like structures, which correspond to different resonant modes of oscillation. We compare this to a power spectrum produced from an above-surface source with observed ridges (left) overlotted.

Power decreases significantly around 5 mHz, in both the model and observations, which corresponds to the acoustic-cutoff frequency ( $\nu_{co}$ ). Waves with frequency higher than  $\nu_{co}$  are non-resonant and dissipate into the solar atmosphere. Sunquakes can generate waves in this frequency range which produce so-called pseudo-modes.

We consider three different types of perturbation: force, velocity, and pressure. We have obtained results for these cases for an above-surface source (spanning from the top of the numerical domain to 300 km above  $R_{sun}$ ) and a below-surface source (from  $R_{sun}$  to 300 km below  $R_{sun}$ ). Time-distance diagrams show little variation with respect to height of source, though the power spectra show marked differentiation (figure 4).

Below-surface perturbations fail to induce strong pseudo-mode oscillations, clearly seen by the lack of power in frequencies greater than 5 mHz. The effects of this can be seen in figure 2, as the below-surface case produces waves with noticeably weaker amplitude than the above-surface case.

Figure 3: Propagation of an acoustic wave through the Solar interior. At T+38 minutes (left), the wavefront still retains a circular shape. At T+63 minutes (right), the wavefront is severely distorted as it travels through the center of the Sun. Faster sound speeds in the interior cause the shallower parts of the wave to lag behind.

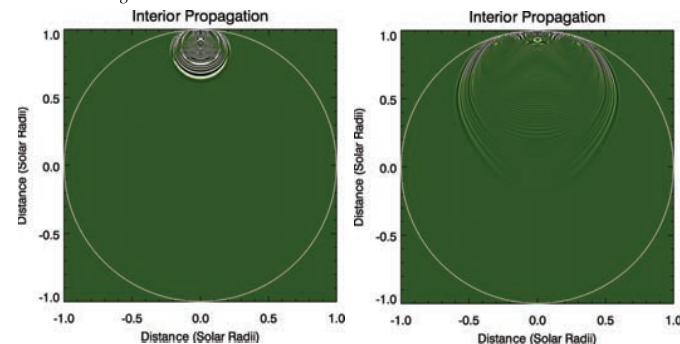
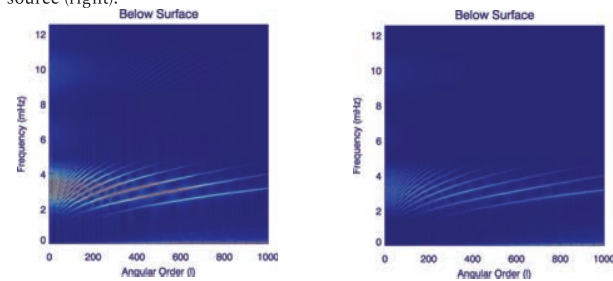


Figure 4: l-v diagram for an above-surface source (left) and below surface source (right).



### DISCUSSION

Preliminary results suggest sunquakes are excited above the solar surface. Other studies (Judge et al, 2014; Martinez Oliveros et al, 2012) have come to similar conclusions; Martinez Oliveros et al analyze height of peak HXR and white light emission, strong indicators of flare heating, to be near 305 and 195 km respectively. It is unlikely that the acoustic source penetrates into the deep photosphere.

Continuing with this work, we plan to perform a parametric study to more precisely examine the effect of perturbation type on propagation. A force perturbation is the most likely candidate for the source, as this type of propagation (figure 5) most closely resembles what we observe, though a velocity (momentum) perturbation is also likely.

Figure 5: Time-distance diagrams for a velocity perturbation (left) and a force perturbation (right). Both sources are above-surface.

